

Self-Assembly of Poly(1,1-diethylsilabutane)-*block*-poly(2-hydroxyethyl methacrylate) Block Copolymer. 2. Monolayer at the Air–Water Interface

Minoru Nakano, Masaki Deguchi, Hitoshi Endo, Kozo Matsumoto, Hideki Matsuoka, and Hitoshi Yamaoka*

Department of Polymer Chemistry, Kyoto University, Kyoto 606-8501, Japan

Received December 23, 1998; Revised Manuscript Received June 25, 1999

ABSTRACT: A spread monolayer of the amphiphilic block polymer poly(1,1-diethylsilabutane)-*block*-poly(2-hydroxyethyl methacrylate) (poly(SB-*b*-HEMA)) on the water surface was investigated by X-ray reflectivity (XR) measurements. Clear Kiessig fringes were observed up to the third order in the XR curve. This observation means the formation of the smooth-faced monolayer with high uniformity of thickness. The thickness of the monolayer increased with increasing surface pressure. Model fitting with the two-layer model revealed that the upper layer is formed by the melt of the SB chains and that the lower layer consists of hydrated HEMA chains. The flexibility of the SB chain is thought to be an origin for the formation of the smooth, dense, and variable-thickness polymer monolayer on the water surface.

Introduction

Adsorption of polymers at the interface plays a very important role in the stabilization and flocculation of colloidal dispersions.¹ In the case of block copolymers in solution, they adsorb at the surface when insoluble segments favorably interact with the surface. In addition to the many reports on the copolymer adsorption to the solid–liquid interface,^{2,3} and for the lipid monolayers at the air–water interface,⁴ the importance of block copolymers at the air–liquid interface is currently increasing. For example, An et al. have performed neutron reflectivity (NR) measurements for absorbed water-soluble block copolymers, poly(2-(dimethylamino)-ethyl methacrylate)-*block*-poly(methyl methacrylate), at the air–water interface and investigated the effects of polymer concentration, pH, ionic strength, and polymer composition.^{5–7} Kent et al. have shown a parabolic concentration profile of polystyrene chains in good solvent tethered to the surface gives the best fit to NR curves for poly(dimethylsiloxane)-*block*-polystyrene at the air surface of ethyl benzoate.⁸ Zhu et al. have revealed the formation of two-dimensional micelles (surface micelle) of polystyrene-*block*-poly(*N*-decyl-4-vinylpyridinium iodide) at the air–water interface and their polymorphism depending on the polymer composition by transmission electron microscopy.^{9,10} Li et al. have investigated the detailed structure of their surface micelles ordered into a quasi-two-dimensional array using both specular and off-specular X-ray reflectivity (XR) techniques and atomic force microscopy.¹¹ Ahrens et al. have used a system of poly(ethyl ethylene)-*block*-poly(styrenesulfonic acid) at the air–water interface and found that the hydrophobic part is a nanometer-thick melt, while the polyelectrolyte forms an osmotically swollen brush of constant thickness independent of grafting density by XR.¹²

Recently, we constructed a compact air–water interface X-ray reflectivity apparatus for laboratory use.^{13–15} This can be a powerful method to investigate the nanostructure at the air–water interface, from the point

of view that the electron density profile of the monolayer normal to the surface can be analyzed *in situ* by specular experiments. In addition, this apparatus has a Langmuir–Blodgett (LB) trough at the sample position, which enables to study the structure of the monolayer as a function of the surface pressure, directly. By using this apparatus, we have been performing systematical XR study for amphiphilic diblock copolymer monolayer,^{16,17} photosensitive amphiphilic graft polymer monolayer,¹⁸ lipid monolayer–DNA complex,¹⁹ and lipid monolayer–protein complex²⁰ at the air–water interface.

Previously, micelle formation of poly(1,1-diethylsilabutane)-*block*-poly(2-hydroxyethyl methacrylate) in selective solvents (methanol and toluene) was described by means of small-angle X-ray scattering,²¹ which showed the spherical micelle formation of the copolymer in methanol and the micelle–unimer–reversed micelle transition with increasing toluene content of methanol/toluene mixed solvents. Although the polymer is insoluble in water, it is expected to form a stable monolayer at the air–water interface. Here, we examine the spread monolayer of this copolymer on the water surface by X-ray reflectivity (XR) measurements. It has been found that this block copolymer forms a uniform-thickness monolayer with a rather smooth surface.

Experimental Section

Sample. Poly(1,1-diethylsilabutane)-*block*-poly(2-hydroxyethyl methacrylate) (poly(SB-*b*-HEMA), see Figure 1) was synthesized as described previously.^{21,22}

The number-averaged degrees of polymerization of SB (*m*) and HEMA (*n*) of the copolymer were determined by ¹H NMR to be 26 and 24, respectively. The polydispersity index M_w/M_n obtained by GPC with CHCl₃ as an eluent was 1.20, where M_w and M_n are the weight- and number-averaged molecular weights, respectively. The copolymer was finally given as a white precipitate by dialysis with deionized water, which was filtered out and lyophilized.

Film Balance Measurement. The surface pressure (π)–surface area (*A*) isotherm of a spread monolayer was obtained by an LB trough (length 600 mm \times width 150 mm) made of aluminum coated by Teflon equipped with a Film Balance

* To whom correspondence should be addressed.

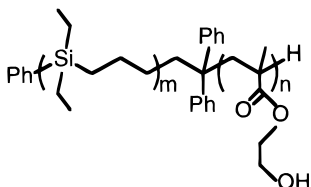


Figure 1. Chemical structure of poly(SB-*b*-HEMA) block copolymer.

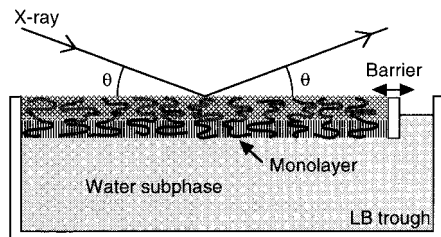


Figure 2. Schematic representation of XR measurement of monolayer at the air-water interface. LB trough mounted on the sample stage of XR apparatus makes possible the XR measurements of monolayer with a change of the surface pressure.

Controller FSD-220 (USI System, Fukuoka, Japan). The water used as subphase was ultrapure water, which was purified and deionized with a Millipore Milli-Q system (≥ 18.2 M Ω resistivity). The copolymer was first dissolved in chloroform to make a 1.1 mg/mL solution and then spread on the water surface by a microsyringe to prepare a monolayer. Thirty minutes was allowed for solvent evaporation before surface compression was started. The measurement was performed at 29 °C. The surface area was compressed by moving a Teflon barrier at the rate of 0.1 mm/s.

X-ray Reflectivity (XR) Measurement. The XR measurements were performed by a RINT-TTR-MA (Rigaku Corp., Tokyo, Japan) which was constructed by a modification of the RINT-TTR θ - θ rotating anode X-ray system for reflectivity measurements. The details of the XR apparatus and data treatment have been fully described previously.^{14,15} The advantage of this apparatus is that in situ measurement of the monolayer at the air-water interface is possible since the sample stage does not move and is kept horizontal during measurement. In addition, an LB trough (length 80 mm \times width 60 mm) made of Teflon (USI System, Fukuoka, Japan) is mounted on the sample stage, which makes possible the XR measurements of a monolayer while changing the surface pressure as schematically shown in Figure 2. The wavelength of the incident X-ray (λ) is 1.5406 Å (Cu K α_1). The measurements were performed under specular condition; i.e., the incident and reflection angles were equal (θ). The reflectivity was obtained as a function of the scattering vector q ($=4\pi \sin \theta/\lambda$).

The LB trough for XR was washed by chloroform and methanol before the water was fulfilled. The cleanliness of the water surface was confirmed by obtaining a satisfactory isotherm of the clean water surface. The chloroform solution of the copolymer that was used for the π - A measurement was spread on the water surface to prepare a monolayer. The XR profiles were obtained at 29 °C at the surface pressures of 25, 35, and 45 mN/m. Each XR measurement took about 1 h to obtain the whole profile. During XR measurement, the position of a Teflon barrier was automatically controlled to keep the constant surface pressure required. The position of the barrier, i.e., the surface area, was monitored during measurements.

Calculations and data analysis for XR were made using a scientific software program invented by Rigaku Corp. and the scientific program "MUREX118 (Multiple Reflection of X-rays)".²³ The procedure of data fitting and simulation is based on the theory of Parratt²⁴ and Sinha et al.²⁵ The details of data treatment and analysis were fully described in our previous papers.^{16,17}

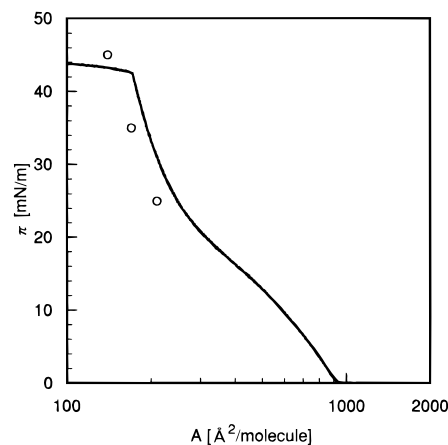


Figure 3. Isotherm of surface pressure versus mean molecular area for spread monolayer of the copolymer ($m:n = 26:24$). Open circles indicate the conditions where XR measurements were performed.

Results and Discussion

The copolymers are insoluble in water since even the polar segment of HEMA itself is insoluble in water. On the other hand, copolymers that have water-soluble segments and form micelles in water cannot form a stable monolayer, because the polymer molecules on the surface easily move into solution under thermodynamic equilibrium. An "appropriate" affinity of HEMA to water, which is enough to make the molecules homogeneously spread on the water surface but not enough to be dissolved or form micelles, gives rise to a possibility of the formation of a stable monolayer on the water surface.

The π - A isotherm of the monolayer of the copolymer is shown in Figure 3. Indeed, the monolayer was stable and was not broken down until the surface pressure reached 42 mN/m. From the isotherm, conformational information on the polymer could be extracted: On compression, the surface pressure starts to increase at ca. 900 Å²/molecule of the surface area, where copolymers adsorbed at the interface contact with each other. At high surface pressures (>25 mN/m), the polymers form a three-dimensional structure, where HEMA chains are stretched and packed inside the water subphase, tethered at the surface by the SB block. In this region, the surface pressure rapidly increases with the reduction of surface area. At the low surface pressure region, the surface pressure gradually increases with compression, where the morphological change from flattened conformation (two-dimensional structure) to the three-dimensional structure proceeds. However, a clear transition regime could not be observed compared with the case of poly(styrene)-poly(ethylene oxide) diblock copolymers, which showed a pseudoplateau regime in the π - A isotherms corresponding to the pancake to quasi-brush transition.²⁶ This is considered to be due to the relatively low molecular weight of the copolymer used in this study, and the polymer with higher molecular weight could show the plateau in the π - A isotherms as predicted by Israelachvili.²⁷

The XR measurements were performed for the copolymer monolayer at the surface pressures of 25, 35, and 45 mN/m, which corresponds to the surface areas per molecule of 210, 170, and 140 Å², respectively, as marked by open circles in Figure 3. In this measurement region, the copolymers are considered to have a three-

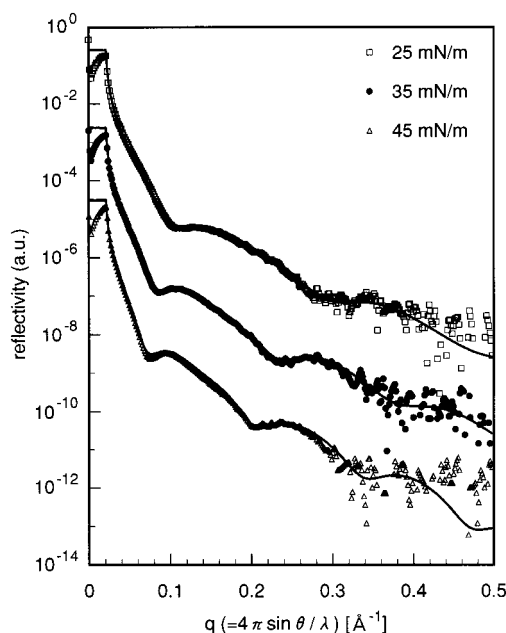


Figure 4. XR profiles of spread monolayer of the copolymer ($m:n = 26:24$) at different surface pressures. Solid lines are fitting curves with the parameters listed in Table 1.

Table 1. XR Results of Monolayer of the Copolymer ($m:n = 26:24$) at the Air–Water Interface

π [mN/m]	A [Å ² /molecule]	d_1 [Å]	d_2 [Å]	σ_1 [Å]	σ_{12} [Å]	σ_2 [Å]
25	210	33	27	3.2	4.1	6.0
35	170	42	35	3.3	4.1	7.5
45	140	47	43	4.0	4.0	8.5

dimensional structure as presumed from π – A isotherm. The XR profiles are shown in Figure 4. For clarity, the curves are shifted down by 2 decades with respect to each other. Clear Kiessig fringes²⁸ were observed up to third order, which represents a uniform thickness and smooth surface of the monolayer. With increasing surface pressure, these fringes shifted toward smaller angles, indicating the increase of the thickness of the monolayer. Specular XR data give the structural information normal to the surface; i.e., we can obtain the electron density profile of the measured layers by model fitting of XR data. We applied the two-layer model in which the upper layer (first layer) is composed of SB and the lower layer (second layer) consists of hydrated HEMA. The electron density of the first layer was fixed to 0.280 Å^{-3} , which corresponds to that of SB, and that of the second layer was varied during fitting which must be between 0.396 (HEMA) and 0.334 (H_2O). The thickness of the first (d_1) and the second layers (d_2), the surface roughness of air–first layer (σ_1), first layer–second layer (σ_{12}), and second layer–water (σ_2) interfaces were adjustable parameters, where roughness is introduced as a standard deviation of Gaussian distribution function to take into account the density smearing at the interface.²⁵ XR profiles were well fitted as can be seen in Figure 4 using the parameters listed in Table 1. The electron density profiles at different surface pressures are shown in Figure 5. Both d_1 and d_2 increased with the increase of the surface pressure. From a thermodynamic aspect, the surface roughness should be small to reduce the surface free energy. Indeed, the obtained σ_1 and σ_{12} were small enough compared with d_1 and d_2 . In addition, the clear interface

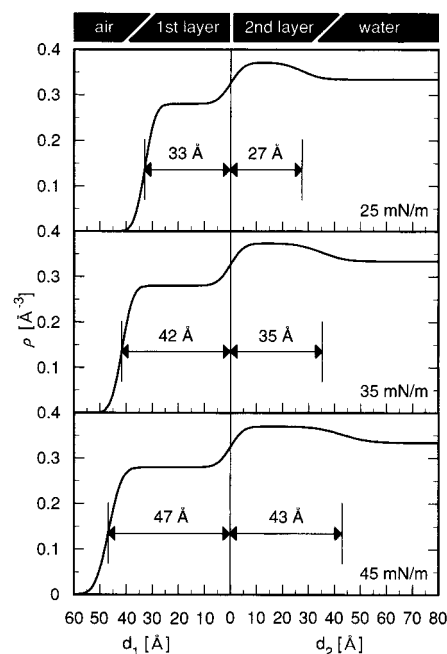


Figure 5. Electron density profiles of monolayer at different surface pressures obtained by fitting of XR data.

between two layers (i.e., small σ_{12}) suggests the high incompatibility between SB and HEMA. On the other hand, σ_2 was relatively larger than σ_1 or σ_{12} , which may indicate that the interface is diffused by the penetration of water to the HEMA layer due to the hydration.

Actually, π – A values of these three conditions did not exactly correspond to the π – A isotherm as shown in Figure 3, and $\pi = 45 \text{ mN/m}$ could not be achieved in the π – A isotherm. On each XR experiment, the surface area was gradually decreasing while the surface pressure kept constant. The surface areas (A) listed in Table 1 are the mean values between onset and end of the XR measurement. We use these values for further discussion (see below). The variation of the surface area during the XR measurement was at most 5% of the mean surface area. Regarding this kind of observation, Kent et al., who have used a PDMS–PS/ethyl benzoate system, have suggested the possibility that some of the copolymer molecules are lost into the bulk of the solution during spreading, since ethyl benzoate is a good solvent for PS.⁸ In our system, however, this cannot happen since water is not good solvent for polar HEMA chains. It is natural to consider that a kind of “rearrangement” of the polymer took place under the constant surface pressure condition, which reduced the surface area and made the monolayer more stable which did not break down even at 45 mN/m . In the case of lipid monolayer, the surface area is reduced while the surface pressure is kept constant which is known as “creep”. The discordance of the π – A values could be reflecting the viscoelastic character of the monolayer,^{4,29,30} although the mechanism is unclear.

The use of many adjustable parameters during the fitting procedure often causes a serious problem; that is, different values of the parameters reproduce a similar profile for the data in which the fringes are not so clear. However, we obtained good fitting results because the clear fringes in these experimental curves enhance the reliability of the fitting. We used the obtained values for the quantitative evaluation as follows:

In all cases, the product of Ad_1 (A is the surface area per molecule at the condition where XR measurement was performed) was $6810 \pm 130 \text{ \AA}^3$, which was in agreement with the volume of an SB chain ($m\nu_{\text{SB}} = 6680$, where m and ν_{SB} denote the volume of repeat unit and the degree of polymerization of SB, respectively, and if the volumes of the terminal phenyl group and hydrocarbon spacer between the two blocks are incorporated, the volume will be 7190) within the experimental error. From this fact, it can be concluded that the first layer is formed by the melt of SB chains, and no density change or transition such as crystallization on increasing surface pressure takes place. The liquid-like state of the first layer is also confirmed from the fact that d_1 is much smaller than the contour length of SB chain (ca. 130 \AA), indicating that SB chains are not highly oriented. Another piece of evidence was obtained by differential scanning calorimetry measurement of a poly(SB) homopolymer with the same molecular weight as the SB segment of the block copolymer, which showed that the poly(SB) was in a melted state at room temperature and had no crystallization point in the temperature range from -100 to $100 \text{ }^\circ\text{C}$.

As for the second layer, $Ad_2 = 5880 \pm 260$, which was almost independent of surface pressure, was larger than the volume of a HEMA chain ($n\nu_{\text{HEMA}} = 4180$, where n and ν_{HEMA} denote the volume of repeat unit and the degree of polymerization of HEMA, respectively). This discordance can be understood if one considers the second layer containing water. Assuming that the difference of the volume corresponds to the volume of water in the layer, the volume fraction of water in the second layer (ϕ_w) was calculated to be $29 \pm 3\%$. ϕ_w can be also calculated from the electron density; that is, the electron density of the second layer (ρ_2) is given with ϕ_w and the electron densities of HEMA and water:

$$\rho_2 = 0.334\phi_w + 0.396(1 - \phi_w)$$

Using the obtained values of ρ_2 by the fitting ($0.371 \pm 0.002 \text{ \AA}^{-3}$), ϕ_w was estimated to be $40 \pm 3\%$. Although there is a small difference in the volume fraction of water calculated by the two methods, the value calculated from the volume could be more reliable since the effect of the length is more sensitive on a theoretical curve than that of the electron density.

Baltes et al. have reported that hydrophobic polymers with low glass transition temperature and a single ionic headgroup form rather thick monolayer films and that the thickness is inversely proportional to the area per headgroup.³¹ The present copolymer also showed the inverse proportions of both first and second layers with the molecular area. It is therefore possible to control the thickness of monolayer by changing the surface area. Preparation of thicker monolayer could be possible with the copolymer of higher molecular weight, which is now under consideration.

Conclusions

The monolayer of poly(SB-*b*-HEMA) amphiphilic block polymer spread on the water surface was investigated by the in situ XR technique. The XR profiles showed very clear Kiessig fringes up to third order. The XR curves showed excellent agreement with theoretical curves obtained by a two-layer model, the upper layer of which is formed by the melt of SB chains and the

lower layer of which consists of hydrated HEMA chains. The thickness of the monolayer increased with increasing surface pressure. The product of Ad_1 was constant and in agreement with the volume of an SB chain. The lower layer was estimated to contain 29% of water by comparison of Ad_2 and the volume of the HEMA chain. These novel amphiphilic copolymers are expected to provide valuable information for theoretical approaches^{32–36} in the surface chemistry as an example that showed various types of self-assembly systems.

Acknowledgment. This work was supported by Grant-in-aid for Scientific Research in Priority Area "New Polymers and Their Nano Organized Systems" (No. 09232230) from the Ministry of Education, Science, Sports, and Culture of Japan. M.N. gratefully acknowledges the support of this work by Research Fellowships of the Japan Society for the Promotion of Science for Young Scientists.

References and Notes

- (1) Fleer, G. J.; Cohen Stuart, M. A.; Scheutjens, J. M. H. M.; Cosgrove, T.; Vincent, B. *Polymers at Interfaces*; Chapman and Hall: London, 1993.
- (2) Guzonas, D.; Boils, D.; Hair, M. L.; Tripp, C. *Macromolecules* **1992**, *25*, 2434.
- (3) d'Oliveira, J. M. R.; Xu, R.; Jensma, T.; Winnik, M. A.; Hruska, Z.; Hurtrez, G.; Riess, G.; Martinho, J. M. G.; Croucher, M. D. *Langmuir* **1993**, *9*, 1092.
- (4) Shah, D. O., Ed. *Micelles, Microemulsions, and Monolayers: Science and Technology*; Marcel Dekker: New York, 1998.
- (5) An, S. W.; Su, T. J.; Thomas, R. K.; Baines, F. L.; Billingham, N. C.; Armes, S. P.; Penfold, J. *J. Phys. Chem. B* **1998**, *102*, 387.
- (6) An, S. W.; Thomas, R. K.; Baines, F. L.; Billingham, N. C.; Armes, S. P.; Penfold, J. *J. Phys. Chem. B* **1998**, *102*, 5120.
- (7) An, S. W.; Thomas, R. K.; Baines, F. L.; Billingham, N. C.; Armes, S. P.; Penfold, J. *Macromolecules* **1998**, *31*, 7877.
- (8) Kent, M. S.; Lee, L. T.; Farnoux, B.; Rondelez, F. *Macromolecules* **1992**, *25*, 6240.
- (9) Zhu, J.; Eisenberg, A.; Lennox, R. B. *J. Am. Chem. Soc.* **1991**, *113*, 5583.
- (10) Zhu, J.; Lennox, R. B.; Eisenberg, A. *J. Phys. Chem.* **1992**, *96*, 4727.
- (11) Li, Z.; Zhao, W.; Quinn, J.; Rafailovich, M. H.; Sokolov, J.; Lennox, R. B.; Eisenberg, A.; Wu, X. Z.; Kim, M. W.; Sinha, S. K.; Tolan, M. *Langmuir* **1995**, *11*, 4785.
- (12) Ahrens, H.; Förster, S.; Helm, C. A. *Phys. Rev. Lett.* **1998**, *81*, 4172.
- (13) Matsuoka, H.; Yamaoka, H. *Proc. Risø Int. Symp. Mater. Sci.* **1997**, *18*, 437.
- (14) Yamaoka, H.; Matsuoka, H.; Kago, K.; Endo, H.; Eckelt, J. *Physica B* **1998**, *248*, 280.
- (15) Yamaoka, H.; Matsuoka, H.; Kago, K.; Endo, H.; Eckelt, J.; Yoshitome, R. *Chem. Phys. Lett.* **1998**, *295*, 245.
- (16) Kago, K.; Matsuoka, H.; Endo, H.; Eckelt, J.; Yamaoka, H. *Supramol. Sci.* **1998**, *5*, 349.
- (17) Kago, K.; Matsuoka, H.; Yoshitome, R.; Mouri, E.; Yamaoka, H. *Langmuir* **1999**, *15*, 4298.
- (18) Kago, K.; Fürst, M.; Matsuoka, H.; Yamaoka, H.; Seki, T. *Langmuir* **1999**, *15*, 2237.
- (19) Kago, K.; Matsuoka, H.; Yamaoka, H.; Ijiri, K.; Shimomura, M. *Langmuir*, in press.
- (20) Yoshitome, R.; Kago, K.; Matsuoka, H.; Yamaoka, H. *Polym. Prepr. Jpn.* **1999**, *48*, 995.
- (21) Nakano, M.; Deguchi, M.; Matsumoto, K.; Matsuoka, H.; Yamaoka, H. *Macromolecules*, in press.
- (22) Matsumoto, K.; Deguchi, M.; Nakano, M.; Yamaoka, H. *J. Polym. Sci., Part A: Polym. Chem.* **1998**, *36*, 2699.
- (23) Sakurai, K. MUREX118: Program for calculation/analysis of X-ray reflectivity, fluorescence intensity from multilayered thin films in grazing incident/exit X-ray experiments. National Research Institute for Metals, Tsukuba, Japan, 1995.
- (24) Parratt, L. G. *Phys. Rev.* **1954**, *95*, 359.
- (25) Sinha, S. K.; Sirota, E. B.; Garoff, S.; Stanley, H. B. *Phys. Rev. B* **1988**, *38*, 2297.
- (26) Gonçalves da Silva, A. M.; Filipe, E. J. M.; d'Oliveira, J. M. R.; Martinho, J. M. G. *Langmuir* **1996**, *12*, 6547.

- (27) Israelachvili, J. *Langmuir* **1994**, *10*, 3774.
- (28) Kiessig, H. *Ann. Phys.* **1931**, *10*, 769.
- (29) Kato, T. *Langmuir* **1990**, *6*, 870.
- (30) Kato, T.; Hirobe, Y.; Kato, M. *Langmuir* **1991**, *7*, 2208.
- (31) Baltes, H.; Schwendler, M.; Helm, C. A.; Heger, R.; Gordel, W. A. *Macromolecules* **1997**, *30*, 6633.
- (32) Alexander, S. *J. Phys. (Paris)* **1977**, *38*, 977.
- (33) de Gennes, P. G. *Macromolecules* **1980**, *13*, 1069.
- (34) Halperin, A.; Tirrell, M.; Lodge, T. P. *Adv. Polym. Sci.* **1992**, *100*, 31.
- (35) Munch, M. R.; Gast, A. P. *Macromolecules* **1988**, *21*, 1360.
- (36) Munch, M. R.; Gast, A. P. *Macromolecules* **1988**, *21*, 1366.

MA9819788